

V.O Kotsyubynsky<sup>1</sup>, V.M. Boychuk<sup>1</sup>, B.I. Rachiy<sup>1</sup>, M.A. Hodlevska<sup>1</sup>, S.I. Budzulyak<sup>2</sup>

## **Structural and Electrophysical Properties of Thermally Expanded Graphite Prepared by Chemical Methods: Comparative Analysis**

<sup>1</sup>Vasyl Stefanyk Precarpathian National University, Ivano-Frankivsk, Ukraine, [kotsyubynsky@gmail.com](mailto:kotsyubynsky@gmail.com)  
<sup>2</sup>V.Ye. Lashkarev Institute of Semiconductor Physics National Academy of Sciences of Ukraine, Kyiv, Ukraine, [buser@ukr.net](mailto:buser@ukr.net)

The aim of this paper is the comparison of structural, morphological and electrical properties of thermally extended graphite synthesized by chemical oxidation of graphite with sulfur or nitric acids at all other same conditions. Thermal treatments of graphite intercalation compounds were performed at a temperature of 600 °C on the air for 10 min but additional annealing in temperature range of 100 - 600 °C for 1 hour was done. The obtained materials were characterized by XRD, Raman spectroscopy and impedance spectroscopy. The evolution of structural ordering of thermally extended graphite samples at increasing of annealing temperature was traced. It was determined that the additional annealing allows to control the electrical conductivity and structural disordering degree of extended graphite samples that is useful for preparation of efficient current collectors for electrochemical capacitors.

**Keywords:** thermally extended graphite, XRD, Raman spectroscopy, electrical conductivity.

*Received 26 October 2020; Accepted 15 December 2020.*

### **Introduction**

Graphite and graphite-based materials have a great spectra of possible application such as hydrogen storage [[1]], electrode material for lithium [[2]] and sodium-ion [[3]] power sources, electrocatalyst [[4]], gas sensors [[5]]. The main reason of graphite polyfunctionality is a peculiarities of its crystal and electronic structure that allow the obtaining of 2D and 3D nanostructured materials like graphene, onion-like carbons or nanotubes. At the same time the large-scale production of than materials is complex and expensive so some relatively cheaper and simpler materials like graphene oxide, reduced graphene oxide and thermally expanded graphite attract great attention especially for electrochemical applications. 2D and quasi-2D materials have a good perspectives for energy storage devices based on the electrochemical intercalation of a Li<sup>+</sup> (or Na<sup>+</sup>) ions into interlayer spacing both in nanoparticles and bulk van der Waals crystals with tunable structural and electric properties [[6]]. Graphite acceptor intercalation compounds with acids (H<sub>2</sub>SO<sub>4</sub> or HNO<sub>3</sub>) are the base for

thermally expanded graphite (TEG) obtaining. The expanded graphite is a high perspective base for electrode of high energy supercapacitor in aqueous electrolytes [[7]]. The main advantages of TEG are the chemically inertness and and high electrical conductivity that depends on the structural and morphological properties of the material with the possibility to form foil without any binder. TEG foil can be successfully used as a support for electrode of electrochemical energy storage device.

The properties of TEG are determined by the details preparation technology that consists in intercalation of acid (mostly H<sub>2</sub>SO<sub>4</sub> or HNO<sub>3</sub>) or salts with its thermal decomposition due rapid. Fast gas evaporation causes the destroying of graphite crystal structure and partial exfoliation of graphene layers with the formation of TEG morphology. The choice of TEG preparation method is crucially important for next electrophysical properties of the materials. In this work a comparative study of structure and electrical conductivity of TEG samples obtained by electrochemical method with different inorganic acids H<sub>2</sub>SO<sub>4</sub> or HNO<sub>3</sub>

## I. Experimental details

### Materials synthesis.

The graphite bisulfate or graphite nitrates were obtained using chemical oxidation of graphite in  $\text{H}_2\text{SO}_4$  (96 %) or  $\text{HNO}_3$  (70 %) aqueous solutions accordingly to protocols described in [[8]]. Synthetic graphite powder (Aldrich, 282863) with average particle sizes less  $20\mu\text{m}$  was used as a raw materials. Oxidation of graphite with acid solution was performed at Teflon vessel under vigorous stirring at  $5^\circ\text{C}$  for 5-6 hours. As a additional oxidizing agent potassium permanganate was used (the mass ratio of graphite powder to  $\text{KMnO}_4$  was 1: 0.15). Graphite powder and potassium permanganate were added to the cooled  $\text{H}_2\text{SO}_4$ , then the obtained mixture was placed in a  $20^\circ\text{C}$  water bath and stirred for 1 hour. The obtained precipitates were separated washed with water several times until the pH of the impregnation solution was about 6.0. Finally, the mixture was slowly dried at  $60 - 70^\circ\text{C}$  for 8 hours. Thermal treatments of graphite intercalation compounds were performed at a temperature of  $600^\circ\text{C}$  on the air for about 10 min. The samples synthesized with sulfur and nitric acids were marked as K1 and K2, respectively. Additional annealing was performed for both samples at 100, 200, 300, 400, 500 and  $600^\circ\text{C}$  for 1 hours.

### Materials characterization.

The structure of the prepared powders were analyzed by XRD (DRON-3M powder diffractometer,  $\text{Cu K}\alpha$  radiation). Raman spectra of were measured with of T64000 Jobin-Yvon spectrometer ( $1800/\text{mm}$ , settling ability of about  $1\text{ cm}^{-1}$ ) in reverse dispersion geometry, using argon-krypton laser ( $\lambda = 488\text{ nm}$ ). Laser irradiation power was less  $1\text{ mW}/\text{cm}^2$  so the local samples overheating was preserved. Chemical composition of obtained materials was investigated by X-ray fluorescence analysis (Expert 3L device, accuracy of determination of chemical elements not less 0.01 mass %). The frequency dependence of electrical conductivity was investigated by impedance spectroscopy (Autolab PGSTAT 12/FRA- 2 device) in the frequency range of 0.01-100 kHz at room temperature. The electrical conductivity was measured for cylindrical samples prepared by pressing at 20 kN.

## II. Results and discussion

XRD patterns of both samples series are presented in Fig. 1, a and b. The XRD pattern for pure graphite is also shown for comparison. The initial graphite show sharp (002) peaks when the samples of thermally expanded graphite additionally show a broad peaks. The angle positions of these peaks doesn't depend on the annealing temperature and are equals of about  $19.5 \pm 0.2^\circ$  and  $18.5 \pm 0.3^\circ$  for samples of K1 and K2 series, respectively. These values correspond to an average d-spacing of 0.454 and 0.479 nm while basal (002) plane interlayer distance for initial graphite sample is 0.334 nm [[9]]. Therefore, the occurrence of (002) peaks in XRD patterns samples after thermal treatment confirms the fact only partial decomposition of intercalated into the

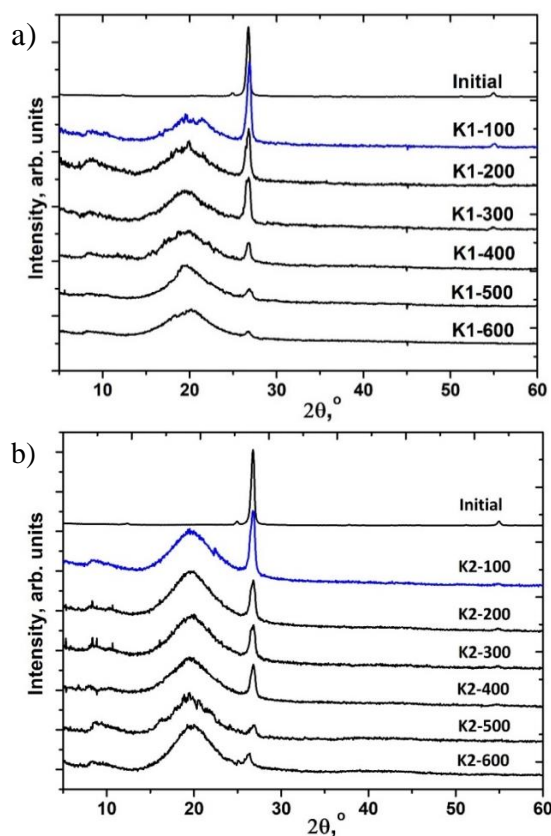


**Fig. 1.** XRD patterns of thermally expanded graphite samples synthesized by intercalation of sulfur (a) and nitric (b) acids after additional annealing at temperature range of 100 -  $600^\circ\text{C}$ .

interlayer spaces of graphite molecules of acids. At the same time the increasing of annealing temperature leads to graphite crystallite sintering and growth of average particle size but this effect is only at temperatures above  $900 - 1000^\circ\text{C}$ [[10]].

The ratio between structurally disordered and not-exfoliated graphite fractions of the samples (amorphization degree) was calculated by the deconvolution of XRD patterns at  $2\theta$ -region of about  $15 - 30^\circ$  to two Gaussian peak with maxima at  $18 - 19^\circ$  ( $\gamma$ -peak) and  $26.7^\circ$  ((002) reflex of graphite structure):  $f_1 = \frac{A_\gamma}{A_\gamma + A_{(002)}}$ , where  $A_\gamma$  and  $A_{(002)}$ -are the integral intensity of  $\gamma$ -peak and (002) reflex, respectively (Fig. 2).

In general, the calculated values of structural disordering degree had a decreasing trend as temperature increased from 100 to  $600^\circ\text{C}$  while K1 samples properties (synthesized with sulfur acids) is respectively higher temperature affected. The samples structural disordering is respectively close after annealing at  $\geq 400^\circ\text{C}$ .

The additional information about structural properties of obtained thermally expanded graphite was obtained using Raman spectroscopy. Typical first-order optical modes Raman spectra of graphite carbon material consist of shows the  $\text{E}_{2g}$  at about  $1580\text{ cm}^{-1}$  that corresponds to the in-phase vibration of the graphite lattice (G band) as well as the additional defect induced peak related to the finite crystallite size (D band) [[11]]. The ratio between D and G bands integral intensity is inversely proportional to the in basal (002) plane

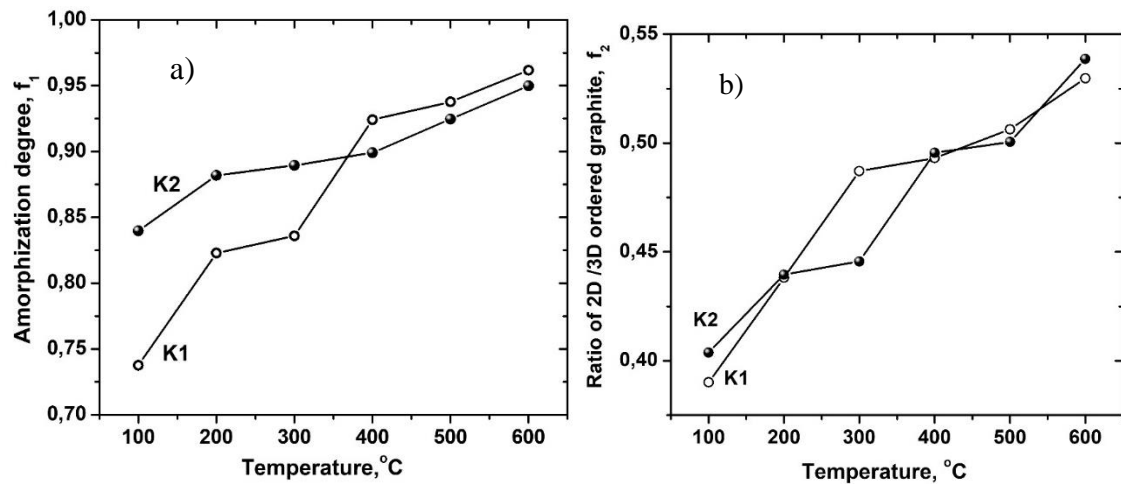


**Fig. 2.** The degree of structural disordering calculated from XRD data (a) and relative content of ratio of 2D /3D ordered graphite calculated from Raman spectroscopy data (b) for thermally expanded graphite samples synthesized by intercalation of sulfur (K1) and nitric (K2) acids as a function of additional annealing at temperature.

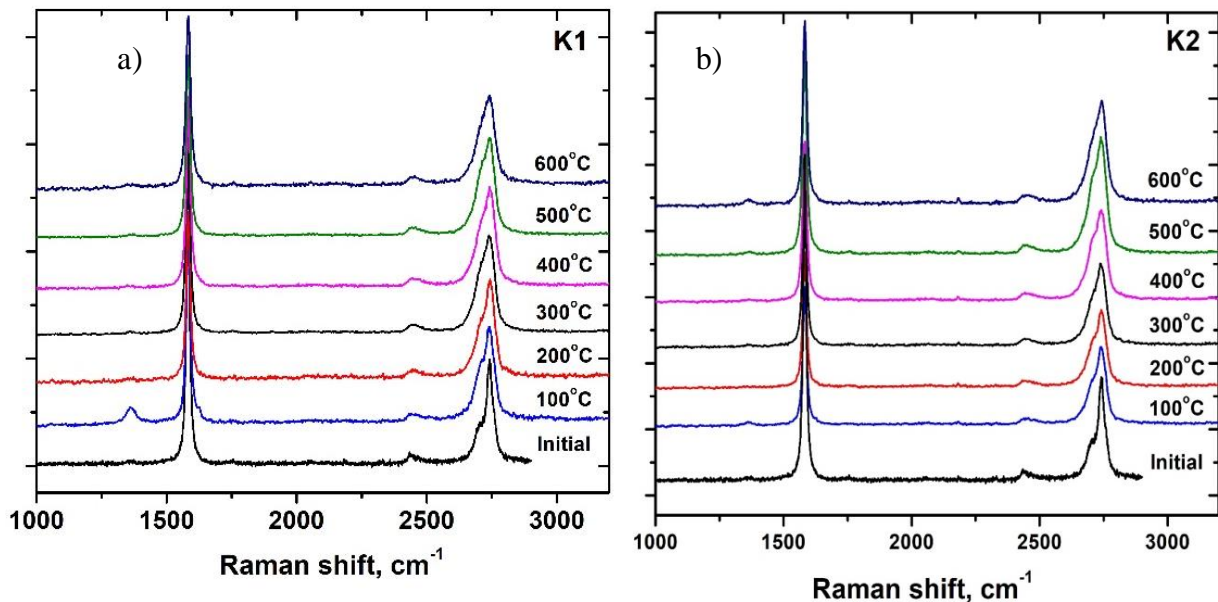


**Fig. 3.** Raman spectra of thermally expanded graphite samples synthesized by intercalation of sulfur (a) and nitric (b) acids after additional annealing at temperature range of 100 - 600 °C.

crystallite size of graphite. Respectively large average in-plane size of crystallite causes the disappearance of D-band for perfect crystals. Experimental Raman spectra obtained for samples of K1 and K2 series don't have D bands. K1-100 sample is only exception but this result is non-systematic.

At the same time the second harmonics of the D bands (called 2D or G' band and located at about  $2700\text{ cm}^{-1}$ ) have an intensity close to G bands [[12]]. This band is sensitive to structural arrangements along the c axes, depending on the number of layers in the packages of turbostratic disordered graphite [[13]]. 2D band of two-dimensional graphite is only single peak at about  $2707\text{ cm}^{-1}$ , but for multilayered packages 2D band is composed by several peaks due to the splitting of  $\pi$  electron dispersion energies as a result of the interaction

between the graphitic planes along the c axes [[14]]. 2D region in a range of about  $15 - 30\text{ cm}^{-1}$  in the Raman spectra of extended graphite samples was deconvoluted using Lorentzian function into its possible constituent peaks. The best fit results were obtained for two components marked  $2D_1$  and  $2D_2$  that correspond to 5 - 6 stacked graphitic layers [[12]]. (Fig. 4). The ratio between relative intensities of  $2D_1$  and  $2D_2$  band is sensitive to the number of graphitic layers and its arrangement in packages. The increasing of disordering degree corresponds to  $2D_2$  band shift upwards that indicates the transition to two-dimensional ordering of graphitic packages formed the turbostratic graphite.

The two stages increasing of  $A(2D_2)/A(2D_1)$  ratio was observed for TEG of K1 series prepared with sulfur

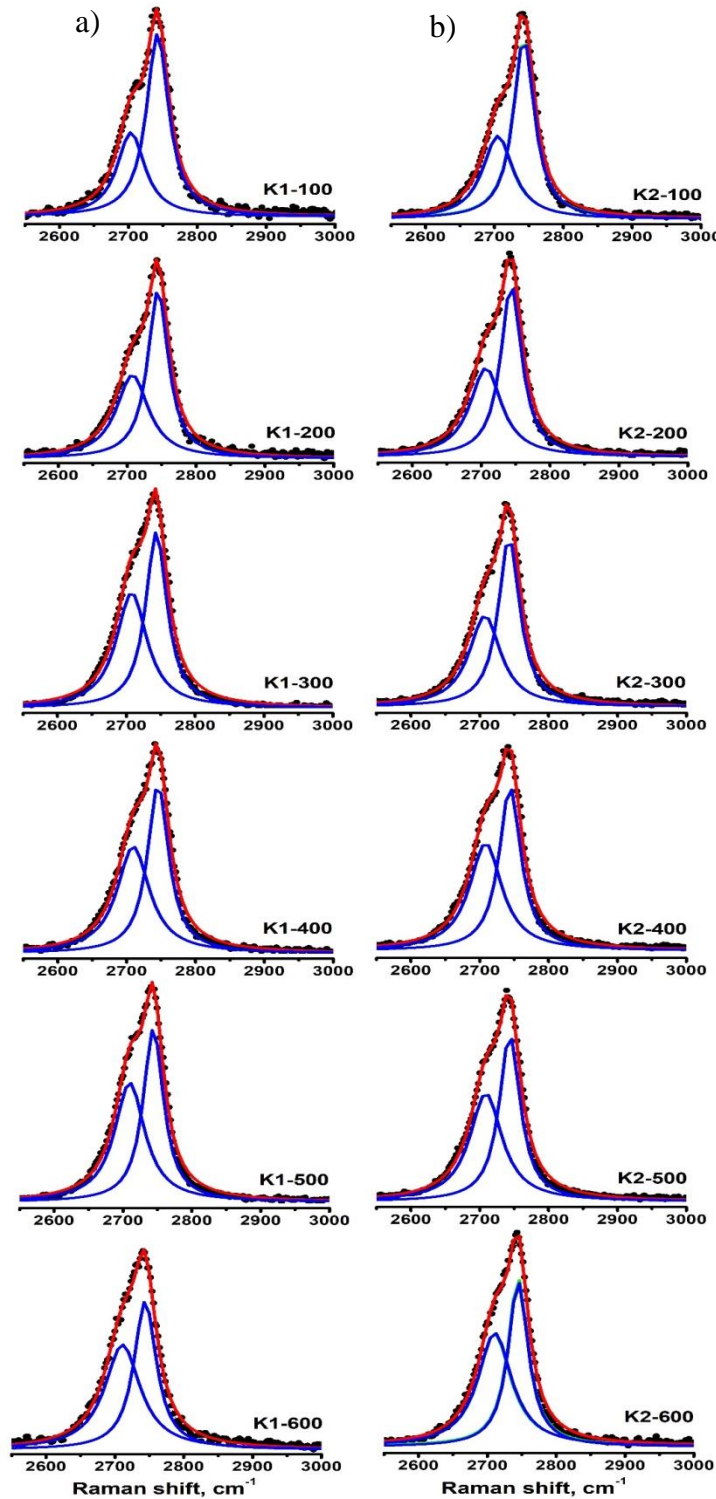


**Fig. 4.** The results of 2D band fitting for K1 and K2 samples series of thermally expanded graphite synthesized by intercalation of sulfur (a) and nitric(b) acids after additional annealing at temperature range of 100 - 600 °C.

acids, while this dependencies for K2 series is only one stage (Fig. 5, a,b). The decreasing of the  $A(2D_2) / A(2D_1)$  ratio changing rate for K1 samples after thermal treatment at  $\geq 300^\circ\text{C}$  is caused by continuation of graphite bisulfate decomposition. the increasing of  $2D_2$  mode intensity is the result the evolution of graphitic planes exfoliation that is the reason the shift of  $2D_2$  peak upwards with respectively stable position of  $2D_1$  peak (Fig. 5, c-d and Fig. 5, e-f). The same results was

observed for 2D band profile of graphite samples with different crystallinity degrees by axes [[14]]. The ratio of 2D and 3D ordered graphite can be estimated from  $2D_2$  and  $2D_1$  peaks intensity as  $f_2 \equiv \frac{A(2D_2)}{A(2D_2)+A(2D_1)}$  (Fig. 2,b). The evolution of  $f_2$  parameters with the increasing of additional thermal treatment temperature is close for samples of both K1 and K2 series. The coordination between XRD and Raman data at annealing temperatures

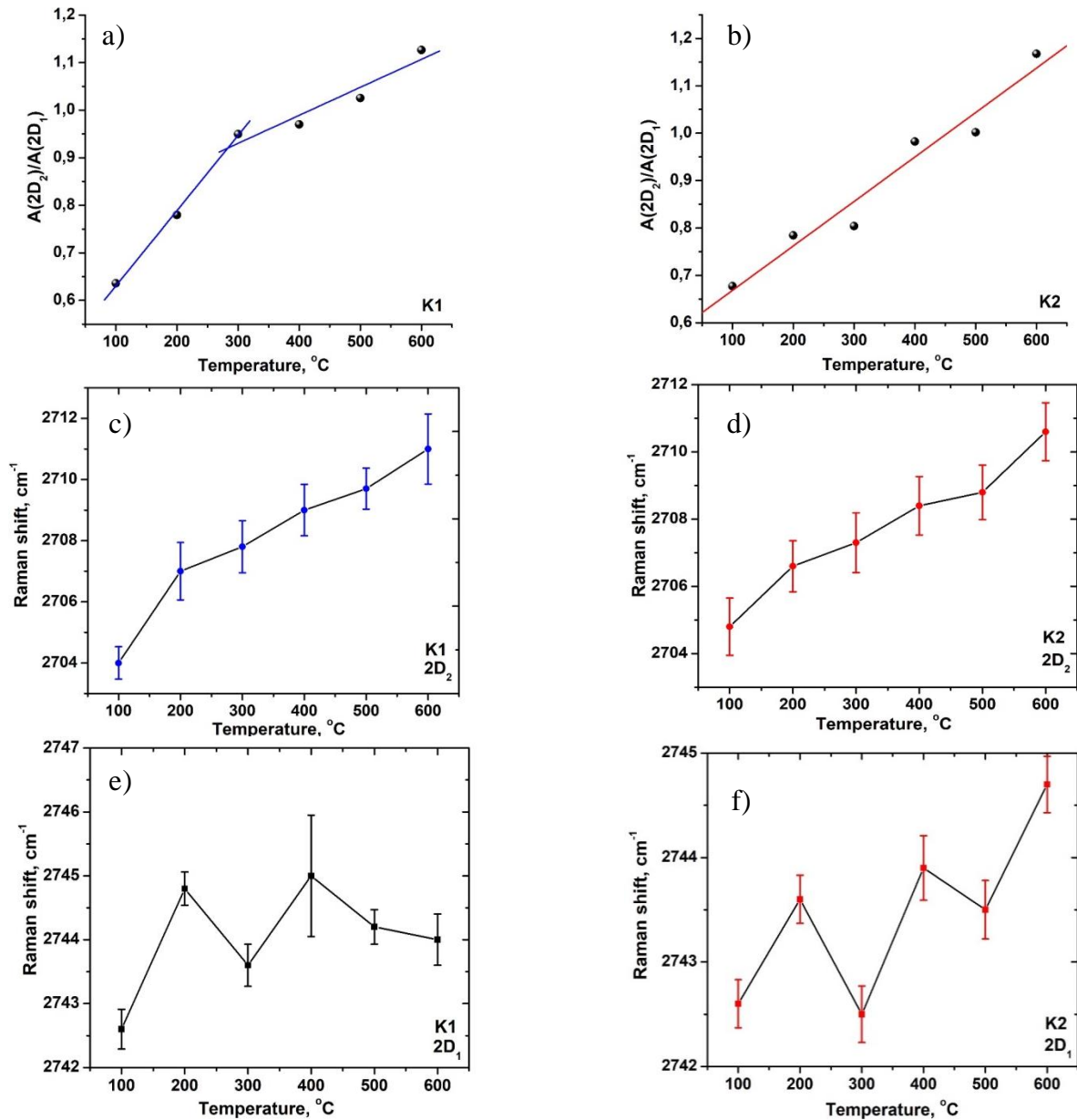


**Fig. 5.** Temperature dependencies of  $A(2D_2)/A(2D_1)$  ratio (a,b) and localization of  $2D_2$  (c,d) and  $2D_1$  (e,f) for K1 and K2 samples of thermally expanded graphite.

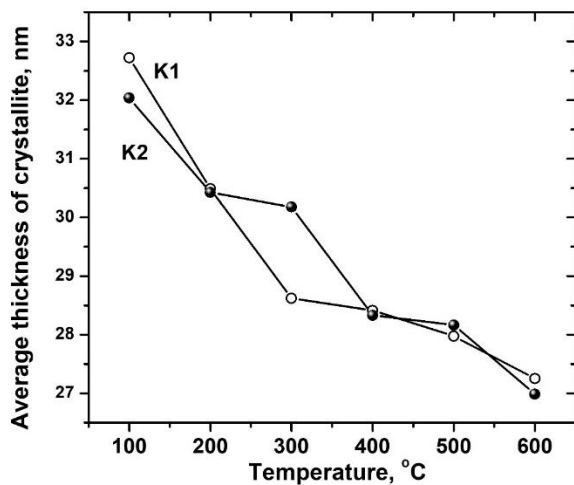


**Fig. 6.** Temperature dependencies of graphite crystallite average for K1 and K2 samples of thermally expanded graphite.

$\geq 400^\circ\text{C}$  indicates that the samples of thermally expanded graphite regardless the type of used at preparation stage acid require additional extended heat treatment at temperatures above  $400^\circ\text{C}$ . An empirical correlation between  $2D/3D$  ordered graphite volume ratio and average thickness of graphites crystallite was proposed in [[14]]:  $L_c(\text{nm}) = 10 + \frac{10}{0.05 + f_2}$ . The calculated values of  $L_c$  for samples of K1 and K2 series are presented in Fig. 6. The very close decreasing character of graphite crystallite average thickness at temperature growth was observed for both samples series in from 32-33 nm to about 27 nm.

The electrical conductivity of obtained samples is almost independent of frequency (Fig. 7, a, b), but varies depending on the thermal treatment conditions (Fig. 7, c). It's clear that the morphology of the obtained materials

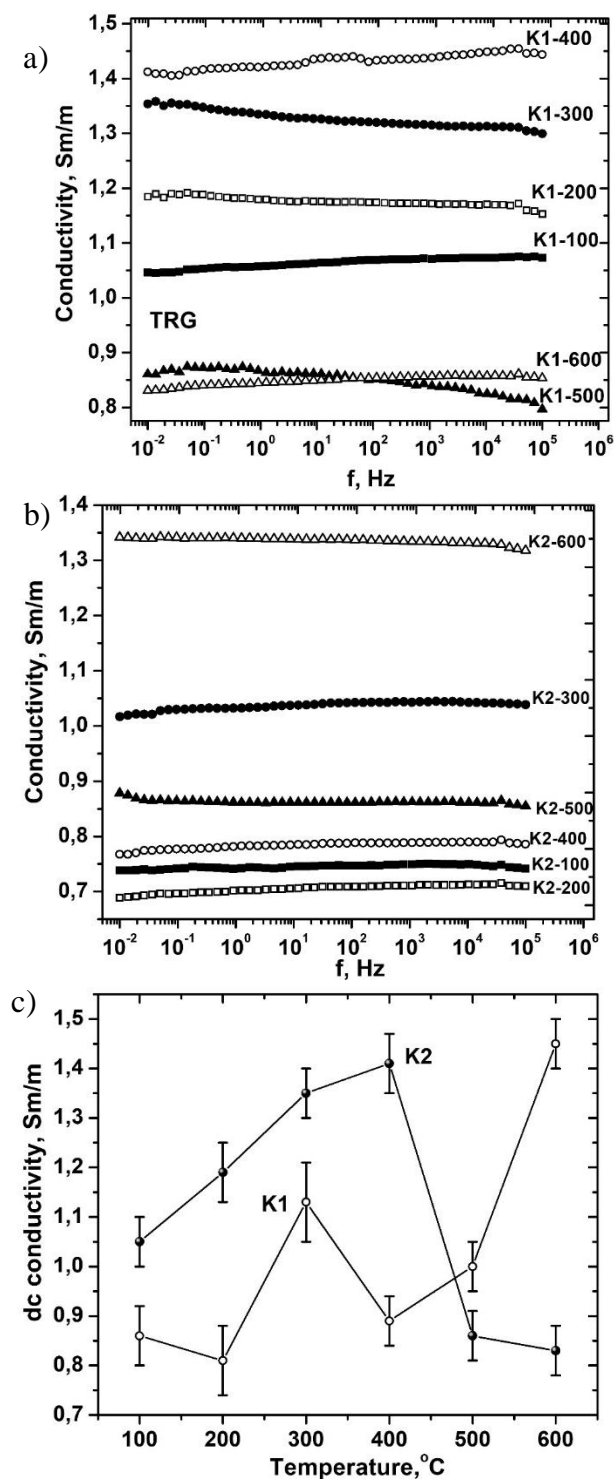


**Fig. 7.** Frequencies dependencies of electrical conductivity for K1 and K2 samples of thermally expanded graphite after additional annealing at temperature range of 100 - 600 °C (a,b) and dc electrical conductivity of these samples as a function of annealing temperature (c).

and presence of characteristics of the ohmic contacts between expanded graphite particles.

Direct current (dc) conductivity of K2 samples has a maxima after thermal treatment at about 400°C with the next decreasing. At the same time dc conductivity for K1 samples has a tendency to increasing with the enlarging of additional annealing temperature.

## Conclusions

The comparative analysis of structural and electrical properties of thermally extended graphite (TEG) samples chemically prepared with sulfur and nitric acids. It was determined that the additional continued annealing (duration 1 h) of TEG samples in a temperature range of 100 - 600 °C allow to complete exfoliation of graphitic planes and effect on the structural ordering of the materials. It was determined that the amorphization degree of TEG samples prepared with sulfur acid is respectively lower but after annealing at the temperatures  $\geq 400$  °C this parameter is about 95 % regardless of used acid type. The analysis of 2D band in the Raman spectra of TEG samples allow to trace increasing the ratio between the volumes of 2D and 3D ordered graphite. An average size of graphite crystallites normally to basal (002) plane decrease from 32 - 33 nm to about 27 nm at annealing temperature increasing in a range of 100 - 600 °C. The electrical direct current conductivity of TEG samples prepared with sulfur acid monotonously increase at annealing temperature enlarging. In summary, obtained results show that current collector for supercapacitors based on the TEG prepared with sulfur acid have an advantages in specific conductivity at condition of additional thermal treatment at 600 °C.

## Acknowledgment

This research was supported by the National Research Foundations of Ukraine (Project No. 2020.02/0043).

**Kotsyubynsky V.O.** – Professor, Doctor of Physical and Mathematical Sciences;  
**Boychuk V.M.** – Professor, Doctor of Physical and Mathematical Sciences;  
**Rachiy B.I.** – Professor, Doctor of Physical and Mathematical Sciences;  
**Hodlevska M.A.** – Ph.D student;  
**Budzulyak S.I.** – Ph.D, senior researcher.

- [1] H. Atsumi, K. Tauchi, Journal of alloys and compounds 356, 705 (2003) ([https://doi.org/10.1016/S0925-8388\(03\)00290-1](https://doi.org/10.1016/S0925-8388(03)00290-1)).
- [2] M. Endo, C. Kim, K. Nishimura, T. Fujino, K. Miyashita, Carbon 38(2), 183 (2000) ([https://doi.org/10.1016/S0008-6223\(99\)00141-4](https://doi.org/10.1016/S0008-6223(99)00141-4)).
- [3] Y. Wen, K. He, Y. Zhu, F. Han, Y. Xu, I. Matsuda, C. Wang, Nature communications 5(1), 1 (2014) ([https://doi.org/10.1038/ncomms5033\(2014\)](https://doi.org/10.1038/ncomms5033(2014))).

- [4] R.R. Moore, C.E. Banks, R.G. Compton, *Analytical chemistry* 76(10), 2677 (2004) (<https://pubs.acs.org/doi/abs/10.1021/ac040017q>).
- [5] S. Drewniak, R. Muzyka, A. Stolarczyk, T. Pustelny, M. Kotyczka-Morańska, M. Setkiewicz, *Sensors* 16(1), 103 (2016) (<https://doi.org/10.3390/s16010103>).
- [6] L.O. Shyyko, V.O. Kotsyubynsky, I.M. Budzulyak, P. Sagan, *Nanoscale research letters* 11(1), 1 (2016) (<https://doi.org/10.1186/s11671-016-1451-4>).
- [7] F. Barzegar, A. Bello, D. Momodu, M.J. Madito, J. Dangbegnon, N. Manyala, *Journal of Power Sources* 309, 245 (2016) (<https://doi.org/10.1016/j.jpowsour.2016.01.097>).
- [8] A.V. Yakovlev, A.I. Finaenov, S.L. Zabud'kov, E.V. Yakovleva, *Russian journal of applied chemistry* 79(11), 1741 (2006) (<https://doi.org/10.1134/S1070427206110012>).
- [9] A.I. Kachmar, V.M. Boichuk, I.M. Budzulyak, V.O. Kotsyubynsky, B.I. Rachiy, R.P. Lisovskiy, *Fullerenes, Nanotubes and Carbon Nanostructures* 27(9), 669 (2019) (<https://doi.org/10.1080/1536383X.2019.1618840>).
- [10] S.C. Wong, E.M. Sutherland, F.M. Uhl, *Materials and manufacturing processes* 21(2), 159 (2006) (<https://www.tandfonline.com/doi/abs/10.1081/AMP-200068659>).
- [11] S. Reich, C. Thomsen, *Philosophical Transactions of the Royal Society of London. Series A: Mathematical, Physical and Engineering Sciences* 362(1824), 2271 (2004) (<https://doi.org/10.1098/rsta.2004.1454>).
- [12] A. Kaniyoor, S. Ramaprabhu, *Aip Advances* 2(3), 032183 (2012) (<https://doi.org/10.1063/1.4756995>).
- [13] X. Zhang, Q. Yan, W. Leng, J. Li, J. Zhang, Z. Cai, E. B. Hassan, *Materials* 10(8), 975 (2017) (<https://doi.org/10.3390/ma10080975>).
- [14] L.G. Cancado, K. Takai, T. Enoki, M. Endo, Y.A. Kim, H. Mizusaki, M.A. Pimenta, *Carbon* 46(2), 272 (2008) (<https://doi.org/10.1016/j.carbon.2007.11.015>).

В.О. Коцюбинський<sup>1</sup>, В.М. Бойчук<sup>1</sup>, Б.І. Рачій<sup>1</sup>, М.А. Годлевська<sup>1</sup>, С.І. Будзуляк<sup>2</sup>

## Структурні та електрофізичні властивості термічно розширеного графіту, отриманого хімічними методами: порівняльний аналіз

<sup>1</sup>ДВНЗ "Прикарпатський національний університет імені Василя Стефаника", м. Івано-Франківськ, Україна, [kotsyubynsky@gmail.com](mailto:kotsyubynsky@gmail.com)

<sup>2</sup>Інститут фізики напівпровідників ім. В.Є. Лашкарева НАН України, Київ, Україна, [buser@ukr.net](mailto:buser@ukr.net)

Метою даної роботи є порівняння структурних, морфологічних та електричних властивостей термічно розширеного графіту, синтезованого хімічним окисленням графіту сірчаною та азотною кислотами. Термічну обробку графітових інтеркаляційних сполук проводили при температурі 600 °С на повітрі протягом 10 хв. з наступним додатковим відпалом в діапазоні температур 100 - 600°С. Отримані матеріали досліджувалися за допомогою X-променевого аналізу, раманівської та імпедансної спектроскопії. Відслідковано еволюцію структури термічно розширеного графіту при підвищенні температури відпалу. Встановлено, що додатковий відпал дозволяє контролювати електропровідність і ступінь структурного впорядкування термічно розширеного графіту та підвищити ефективність струмознімачів для електрохімічних конденсаторів.

**Ключові слова:** термічно розширений графіт, XRD, раманівська спектроскопія, електропровідність.